

Impacts of sagebrush vegetation in a desert climate on the atmospheric boundary layer

Byron Eng, Matthew Moody, and Travis Morrison

April 29, 2017

Abstract

XXX

1 Introduction

2 Results

Data was provided from the Sagebrush and Playa sites for October 18-19th. Both sites harvested data from meteorological towers equipped with fast response sonic anemometers at multiple heights (18.8 m, 10.15 m, 5.87 m, 2.04 m, and 0.55 m for Sagebrush and 25.5 m, 19.4 m, 10.4 m, 5.3 m, 2.02 m, 0.61m for Playa). The variables of interest measured were the three components of velocity (captured at 20 Hz), temperature, relative humidity (captured at 1 Hz). As a post-processing step the analysis, velocity data components were rotated based on 30-minute block averages, with u denoting the mean wind direction, v as the velocity horizontally perpendicular to the mean flow, u , and w as the vertical velocity. Fluctuations from the mean were also calculated from a 30-minute block average.

\bar{u} , \bar{v} , and \bar{w} were calculated using the rotated velocity data. \bar{v} and \bar{w} are close to zero (order of 10^{-4} and 10^{-5} , respectively) for the entire observation period (Figures 1 and 2) verifying that the rotation algorithm performed as expected. Velocity perturbations (u' , v' , and w') were calculated using these mean values. 30-minute block averages and perturbations were also calculated for temperature, T (measured at 1 Hz).

Sensible heat flux (H_s) was calculated for both sites using Equation 1. Where C_p is the specific heat of dry air at constant pressure, and ρ is the density of air.

$$H_s = C_p \cdot \rho \cdot \overline{w'T'} \quad (1)$$

Turbulence kinetic energy (TKE) was calculated for both sites using Equation 2.

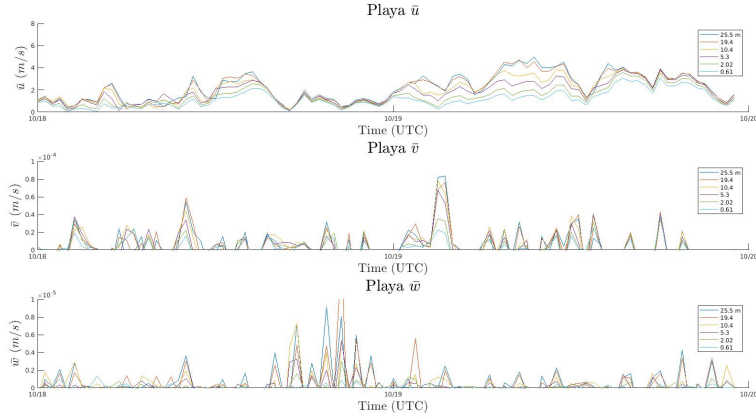


Figure 1: 30-minute block averages of \bar{u} , \bar{v} , and \bar{w} from the Playa.

$$TKE = \frac{1}{2} \overline{u'^2 + v'^2 + w'^2} \quad (2)$$

Figure 3 shows comparisons for H_s and TKE at both sites. Vegetation at the Sagebrush site appears to inhibit sensible heat flux at all observed heights, indicating surface heat storage induced by vegetation. Sagebrush near-surface TKE also appears inhibited by vegetation which is compensated by a sharp TKE increase just above the surface. The Playa site shows a more uniform distribution of TKE at all observed heights.

$$L = \frac{u_*}{\kappa \overline{w'T'}} \quad (3)$$

Equation 3 shows the calculation used for Obukhov length (L), where κ is the Kolmogorov constant (assumed equal to 0.4), and $u_* = \sqrt[4]{\overline{u'w'^2} + \overline{v'w'^2}}$. The time series of L (Figure 4) show that the Playa had more near-surface instability during the observation period. However, approximately 2 meters above the surface L at the Playa remained near zero for the majority of the observation period while L fluctuated between positive and negative with greater amplitude at the Sagebrush site.

To better understand the impacts of vegetation on boundary layer flow, examination of a highly convective time, 1500-1530 MST (2100-2130 UCT), was further analyzed. Characteristics of this period include a mean wind speed and direction of... . The Probability Distribution Function (PDF) for this time period was calculated for each velocity component and temperature at all heights (Figure 5). The largest contrast between the two sites exist between the mean wind velocity component and the temperature. Beginning with u at the sagebrush site the velocity distribution's mean value shifts towards larger values

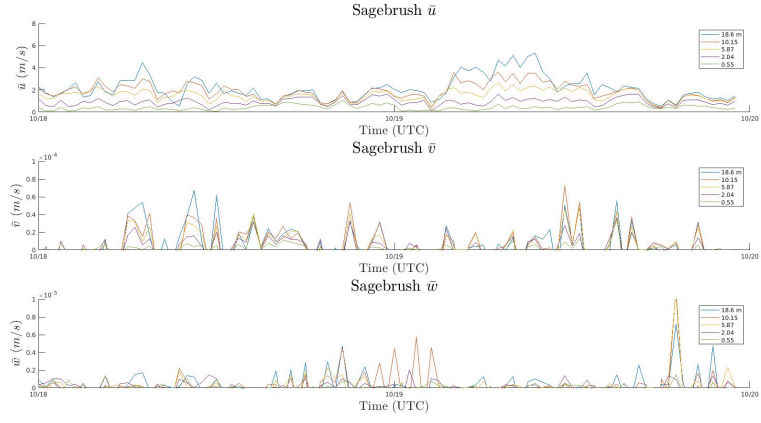


Figure 2: 30-minute block averages of \bar{u} , \bar{v} , and \bar{w} from the Sagebrush site.

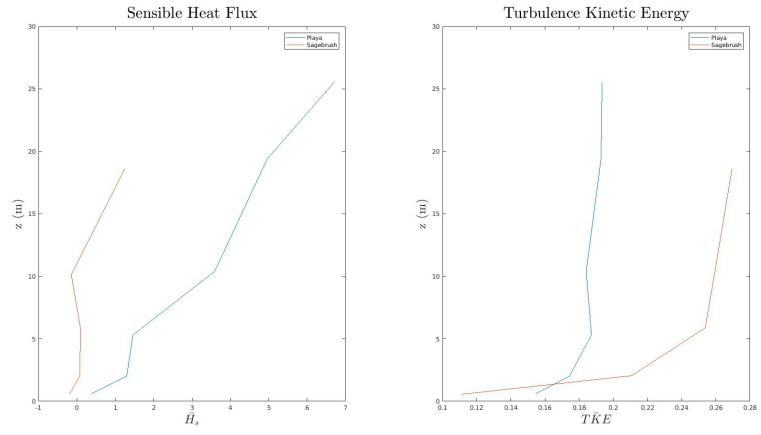


Figure 3: H_s and TKE comparisons. Values at each height were averaged over the observation period.

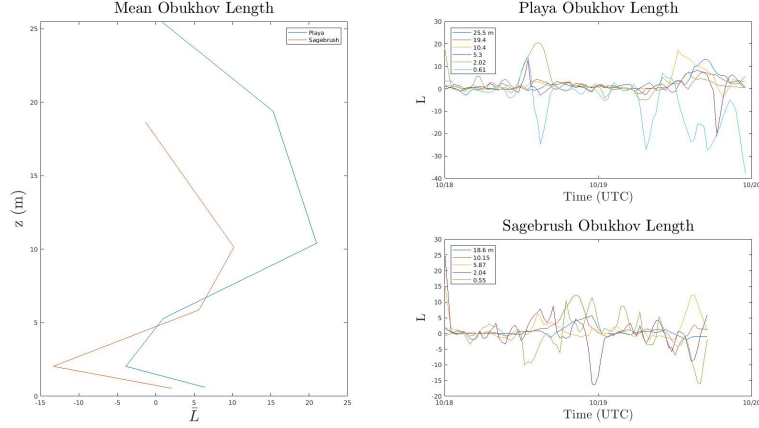


Figure 4: Obukhov length comparison. Mean Obukhov length plotted at each height (**left**), and time series (**right**) for both sites. Time series data were smoothed, giving little weight to outliers, using a variation of Loess Smoothing.

with height, while at the Playa a more uniform mean velocity is maintained with height. Additionally, differences between the temperature PDF's between the two sites can be observed. At the Sagebrush site, the lower two heights (0.55 and 2.04 m) report much larger mean temperature values ($\sim 19.5^\circ \text{C}$) than the other heights ($\sim 19.5^\circ \text{C}$), while at the Playa site, the temperature varies less with height ($\sim 15\text{--}16.5^\circ \text{C}$). Note at the Sagebrush site the temperature PDF at 0.55 m shows the largest variance. These features can potentially be attributed to the vegetation. Due to the low surface vegetation at the Sagebrush site, increased drag reduces the near surface velocity and increases energy storage (higher surface temperature).

It appears the increased mixing at the surface of the Sagebrush creates a more equally well distributed velocity.

Examination of this idea can be further seen in Table 2 and Table 2, where the kurtosis and skewness is presented with height and variable. The red and blue color boxes correlate to the near surface u velocity. At the Sagebrush the skewness nears 0 at the surface, increasing with height and a kurtosis less than 3. While at the Playa, there is a positive skew near the surface, which decreases with height with a decreasing kurtosis. Figure 6 presents the Cumulative Distribution Function (CDF). Focusing on the third row (CDF w) one can now see of the increased distribution of vertical velocities with height at both heights. This is due to the convective nature of the period of interest. Figure 7 presents the autocorrelation function for the velocity components and the temperature at both sites. The autocorrelation was computed for the 30 minutes of interest, 15 minutes is presented. u , v , and T show fairly linearly decays in time, while w decays rapidly to 0. Interesting features in Figure 7 are seen

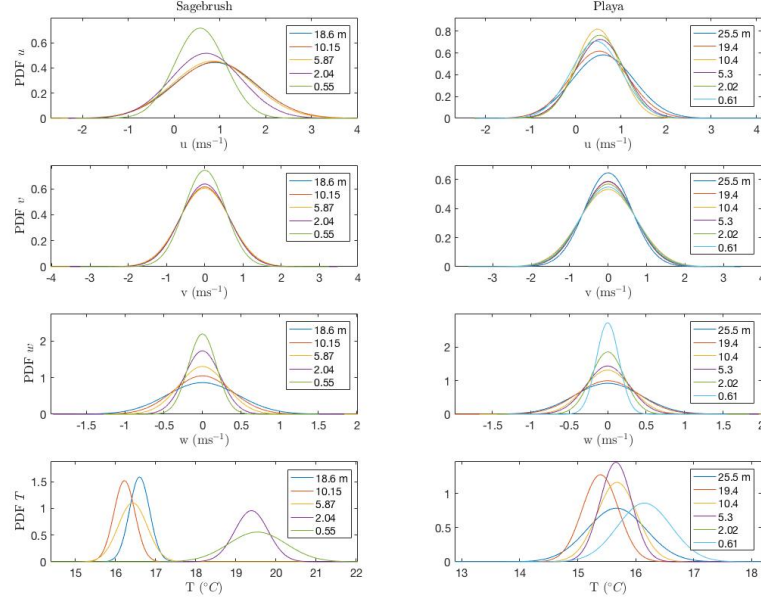


Figure 5: Collection of probability distributions from the Sagebrush (**left**) and the Playa (**right** sites). From top to bottom PDF u , PDF v , PDF w and PDF T .

Sagebrush					
z (m)	Statistic	u	v	w	T
18.6	Kurtosis	2.3731	3.1820	3.6346	1.6588
	Skewness	0.3067	0.2446	0.8532	-0.3490
10.15	Kurtosis	2.4933	3.4515	2.8027	1.8469
	Skewness	0.1651	0.1227	0.3879	-0.5126
5.87	Kurtosis	2.6679	3.2820	3.8053	2.0491
	Skewness	0.2694	0.1717	0.5359	-0.6396
2.04	Kurtosis	2.6868	3.6466	3.3045	2.0662
	Skewness	0.1876	0.3174	0.4101	-0.4458
0.55	Kurtosis	2.6739	3.1869	3.8168	2.4663
	Skewness	0.0655	0.3693	0.3859	0.7037

Table 1: Skewness and kurtosis values for the Sagebrush site on October 19th from 1500-1530 MST.

Playa					
z (m)	Statistic	u	v	w	T
25.5	Kurtosis	2.1075	2.5910	3.5269	2.2656
	Skewness	0.1212	-0.2004	0.7672	0.5295
19.4	Kurtosis	2.2519	2.8332	3.4123	1.6080
	Skewness	0.2287	-0.2862	0.7324	0.1421
10.4	Kurtosis	2.8320	1.9469	3.0079	4.6
	Skewness	0.3884	0.1464	0.3786	1.2276
5.3	Kurtosis	2.9033	2.1528	3.1285	3.2123
	Skewness	0.1862	0.1298	0.4560	0.9190
2.02	Kurtosis	3.0038	2.0993	3.2620	2.3460
	Skewness	0.3980	-0.0969	0.4160	0.6531
0.61	Kurtosis	3.1414	1.9599	3.3634	2.3473
	Skewness	0.5253	-0.1403	0.2770	0.6531

Table 2: Skewness and kurtosis values for the Playa site on October 19th from 1500-1530 MST.

in the autocorrelation of u at the Sagebrush and Playa. At the Sagebrush we observe a more rapid decay of correlation at the lower heights, while at the Playa, all heights remain share the same correlation with time (decrease at the same rate). Additionally, further turbulence analysis was performed on on the data from the two sites. Figure 10 presents the temperature with height (right) of the two sites, while the left column presents (from top to bottom) the mean velocity with height, instantaneous plots of u' , v' , and w' with height. The data presented is only of the period of interest. From the temperature profile, we observe a large energy storage (2°C) at the surface layer compared to the Playa. In the mean velocity we also observe the impact of the sagebrush on the mean flow, creating a large drag at the surface. Examination of the fluctuations reveals the

3 Conclusion

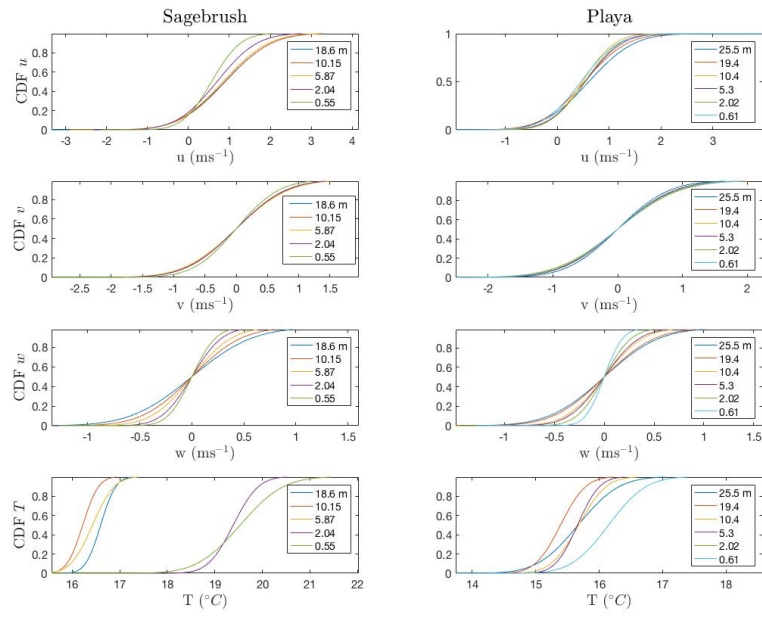


Figure 6:

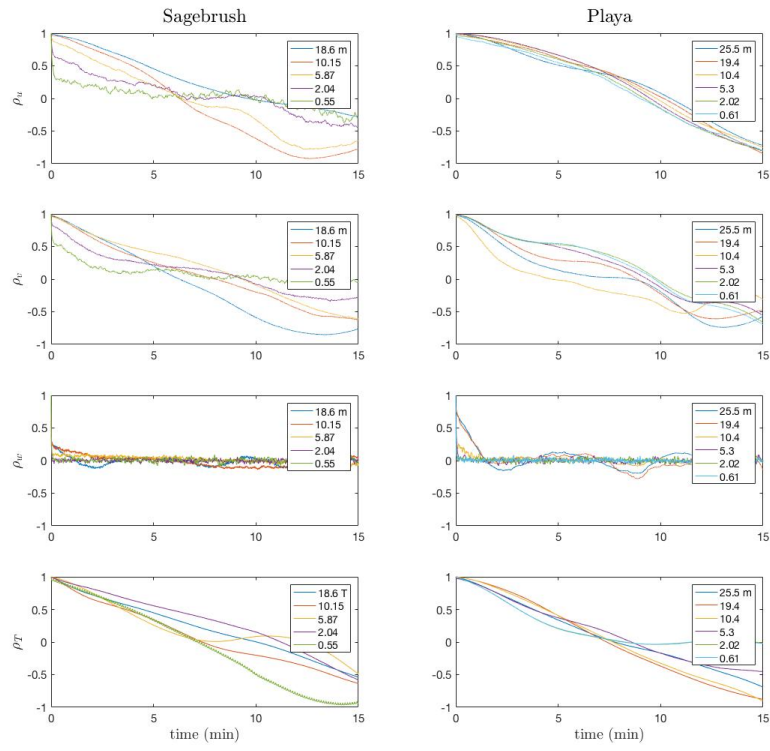


Figure 7:

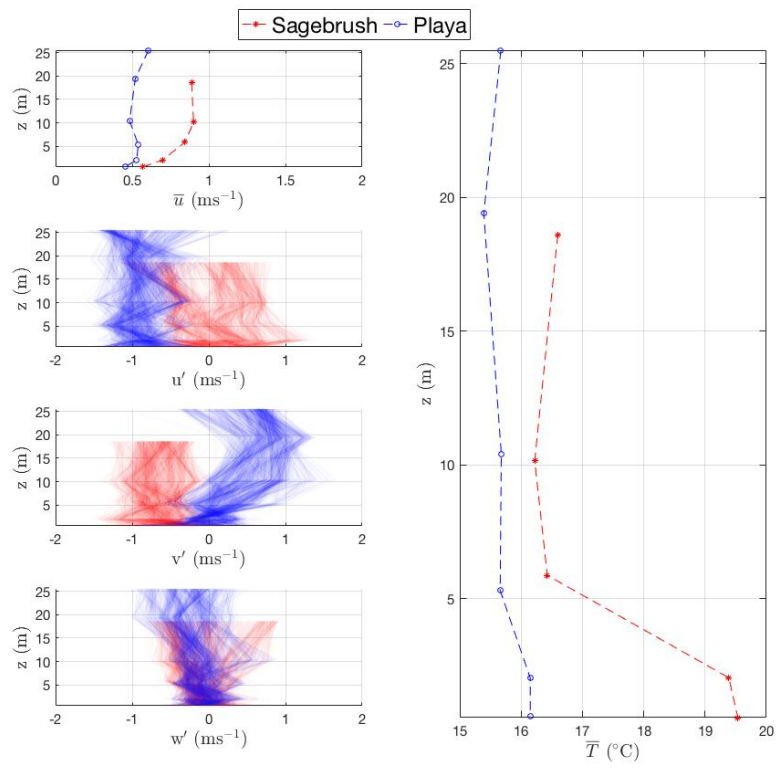


Figure 8:

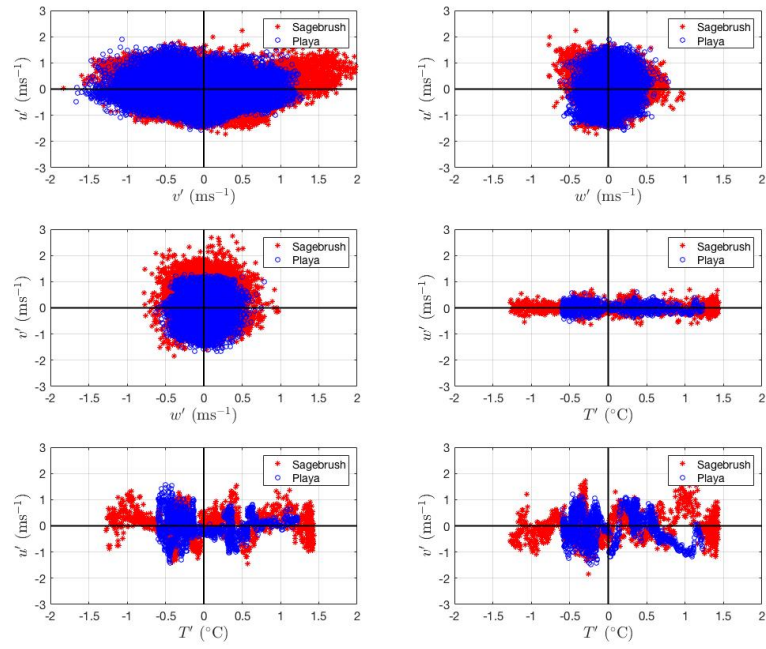


Figure 9:

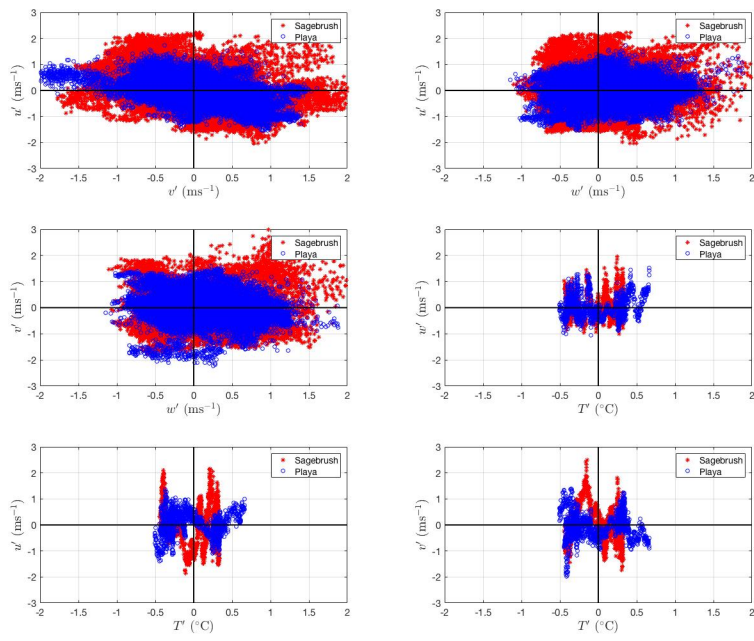


Figure 10: